Cu-catalyzed Si-NWs grown on "carbon paper" as anodes for Li-ion cells

M. Ottaviani, F. Rondino, M. Moreno, L. Della Seta, P. Gislon, V. Orsetti, A. Rufoloni, A. Santoni, P. P. Prosini, and M. Pasquali

View Online   **Export Citation**

ARTICLES YOU MAY BE INTERESTED IN

Cu-Catalyzed Si-NWs Grown on "Carbon Paper" as Anodes for Li-Ion Cells

M. Ottaviani[1a)], F. Rondino[2], M. Moreno[3], L. Della Seta[3], P. Gislon[3], V. Orsetti[2], A. Rufoloni[2], A. Santoni[2], P.P. Prosini[2], M. Pasquali[1]

[1]*SBAI Department "La Sapienza" University of Rome, Via del Castro Laurenziano 7, 00161 Rome, Italy.*
[2]*ENEA, Italian National Agency for New Technologies, Energy and Sustainable Economic Development, Frascati Research Centre, via E. Fermi 45, 00044 Frascati, Italy*
[3]*ENEA, Italian National Agency for New Technologies, Energy and Sustainable Economic Development, Casaccia Research Centre, Via Anguillarese 301, 00123 Santa Maria di Galeria, Rome, Italy.*

[a)]Corresponding author: Michela Ottaviani: michela.ottaviani@uniroma1.it

Abstract. The very high theoretical capacity of the silicon (4200mAh/g more than 10 times larger than graphite), environmental-friendly, abundant and low-cost, makes it a potential candidate to replace graphite in high energy density Li-ion batteries. As a drawback, silicon suffers from huge volume changes (300%) on alloying and dealloying with Li, leading a structural deformation that induces disruption. The use of nanostructured silicon materials has been shown to be an effective way to avoid this mechanical degradation of the active material. In this paper the synthesis of silicon nanowires, grown on a highly porous 3D-like carbon paper substrate by CVD using Cu as the catalyst, is presented. The use of carbon paper allows to achieve remarkable loadings of active material (2-5 mg/cm^2) and, consequently, high capacity densities. The silicon electrode was investigated both morphologically and electrochemically. To improve the electrochemical performance various strategies have been carried out. It was observed that a very slow first cycle (C/40), which helps the formation of a stable solid electrolyte interphase on the silicon surface, improves the performance of the cells; nevertheless, their cycle life has been found not fully satisfactory. Morphological analysis of the Si-NWs electrodes before and after cycling showed the presence of a dense silicon layer below the nanowires which could reduce the electrical contact between the active material and the substrate.

INTRODUCTION

Lithium-ion batteries (LIBs), with their higher energy density and operating voltage, a lower self-discharge and a good power performance compared to conventional Ni-MH or lead/acid batteries, are considered at present the highest-performing available rechargeable batteries [1,2] .They are currently one of the most popular types of batteries for portable electronic devices and, by using the lightest electrochemically active material, lithium, they can store more energy compared to other rechargeable batteries. However, current LIBs seem to have reached their upper limit in volumetric and gravimetric energy densities. The existing LIBs use a combination of graphite-based anode materials and metal oxide or lithium iron phosphate cathode materials in which lithium ions can be easily intercalated. The mechanism based on the intercalation, despite the good capacity retention shown over many cycles, suffers from a relatively low specific capacity (≈ 370 mAh g-1 for graphite and 140-200 mAh g-1 for lithium metal oxide/phosphate) determined by the limited number of available intercalation sites [3,4]. In contrast, materials which form alloys with lithium can exceed the limits shown by materials which intercalate them. Among these, silicon represents the most promising candidate to replace conventional graphite anodes used in LIBs. Silicon has the highest theoretical specific capacity (≈ 4200 mAh g-1) corresponding to the alloy Li22Si5, with 4.4 Li ions inserted per Si atom. As drawback the alloying process causes a huge expansion of the active material ($\approx 300\%$ in volume) which induces a strong mechanical stress in the silicon structure. The reiterative alloying-dealloying process leads to a rapid cracking of the Si structure and to the partial or total loss of the electric contact between the active material and the current collector, which results in a rapid decline in performance [5-7]. Silicon nanostructures, due to their dimensions and morphology, have been proved to prevent the active material degradation guaranteeing a good electrical contact with the current collector. Several different structures such as silicon nanowires (Si-NWs) [5], porous silicon [8] or silicon dispersed in an active/inactive matrix [1,9] have been investigated in different studies. Si-NWs, in particular, have several advantages with respect to the others: the presence of void space between nanowires that can buffer a volume expansion and the one-dimensional structure that facilitates the strain relaxation, withstanding the mechanical stress during cycling and avoiding silicon degradation. Furthermore, Si-NWs are directly connected to the electrode without the use of any binder creating in this way a very efficient pathway for electric charge transport. Finally, this kind of architecture presents the add-on advantage of shorter diffusion distances for Li ions so offering the possibility to increase charging and discharging rates [5-7,10]. Among all Si-NWs, those with a core-shell

structure show a good storage charge capacity even at high cycling rate [11]. The core-shell structure consists of a crystalline silicon core, that enables the electrical transport and represents a very stable mechanical support for the nanowires, and an amorphous silicon shell that can efficiently store Li-ions. Despite the optimistic premises, all the issues connected to the volume expansion during the cycling process and, consequently the capacity fading upon cycling, are still observed, as well as a high irreversible capacity in the first cycle and a low Coulombic efficiency in further cycles. Recently the role of the solid electrolyte interphase (SEI) has emerged as the main cause for the capacity fading and many studies have been devoted to understand its chemical and structural composition in order to create a stable passivation layer on the electrode surface [12-14].In the work of Peled and co-workers [15] a three-dimensional fiber-based substrate (carbon paper) has been used as a conductive network to grow Si-NWs by CVD using Au nanoparticles as a catalyst and a pre-treatment of the substrate by oxygen plasma followed by the adsorption of poly- L-lysine at room temperature has been applied to improve the Si-NWs adhesion. The obtained Si-NWs showed a very low capacity degradation (0.25% during a hundred cycles) very high cycle capacity and a stable cycle life [15]. In this paper the synthesis of Si-NWs on carbon paper substrates, by Cu-catalyzed CVD using pure SiH4 or diluted with Ar as precursor gas is described. The deposition was carried out on substrates with no prior treatment followed by the investigation of the morphological and electrochemical properties of the obtained Si-NWs.

EXPERIMENTAL

Synthesis of Si-NWs

Si-NWs were directly grown on 0.28 mm thick carbon paper (Toray TGP-H-090) by CVD technique [16-17]. This conductive substrate was chosen to reduce the weight of the electrochemically inactive components of the cell to obtain a higher gravimetric energy density, in comparison with a previous work on stainless steel [18]. The area of the substrates was about $1 cm^2$. The substrates were covered with Cu nanoparticles (PlasmaChem), acting as catalyst, using a commercial suspension that provides a known density (6 μg ml^{-1}) and a known diameter (40 nm) of primary nanoparticles. A commercial pneumatic nebulizer for medical use (Chiesi, Clenny A Aereosol) was adopted to spray the suspension onto the carbon substrate, allowing a uniform metallic nanoparticle distribution and preventing nanoparticle agglomeration. The functionalized substrates were then inserted into a quartz tube, using a ceramic container, and placed into a CVD furnace (Lenton, UK). A base pressure vacuum of $1x10^{-4}$ Pa was made inside the growing chamber. Silane, pure or mixed with argon, was used as the silicon precursor. An accurate choice of growing parameters was performed in order to obtain Si-NWs suitable to be used as electrodes in LIBs. The tunable parameters were the pressure of the precursor gas as well as the flow rate and the growing duration. Although the eutectic temperature of Cu/Si alloy required for the Si-NWs growth by VLS mechanism is 802 °C [16-17], the synthesis of Si-NWs can also occur at lower temperatures and this effect may be ascribed to the vapor solid-solid process [19-20]. The Si-NWs weight was accurately determined by measuring the mass of the sample using a microbalance (Sartorius SECURA 125-1S) before and after the growth.

Morphological, Compositional and Structural Characterization

All the samples were morphologically evaluated by using a SEM equipped with EDS for qualitative elemental analysis (Tescan Vega 3 with LaB6 source and Edax Element microanalysis and HR-FEGSEM Leo 1525). The structural composition was also investigated by using an X-ray diffractometer (Rigaku D-max) with Ni filtered CuKα radiation equipped with a curved graphite monochromator on the diffraction beam. Post mortem analysis was performed after electrochemical cycling tests collecting the samples by manually dismantling the coin cells and washing the carbon paper electrodes three times in fresh DMC to remove the residual electrolyte.

Electrochemical Characterization

The Si-NWs samples were directly used as electrodes without adding binders or conducting carbon. Coin-type cells (LIR 2016) were assembled using a 12 mm in diameter Li metal foil as counter electrode and glass fibre (Whatman Grade GF/A) or poly-propylene foil (Celgard 2325) soaked with the electrolyte solution (LP30 Merck, battery grade), as separators. The content of water in the electrolyte was checked by using a coulometric titration (Karl Fischer C20S). A multichannel battery tester (Maccor 4000) was used for the galvanostatic charge-discharge cycling tests. Cyclic voltammetry was carried out with a potentiostat (Solartron 1287). Cell assembly and electrochemical tests were performed in a dry room (R.H.<0.1% at 20 °C).

RESULTS AND DISCUSSION

Silicon nanowires were grown using three different set of parameters (Tab. 1) that led to two main morphologies as shown in Fig. 1 and Fig. 2.

TABLE 1. Different growing parameters used.

Precursor Gas	Flux Rate (sccm)	Precursor Pressure (Pa)	Temperature (°C)	Time (min)
SiH$_4$	6	267	620	12
SiH$_4$+Ar	1+10	800	620	24
SiH$_4$+Ar	2+10	800	620	24

The use of pure SiH$_4$ gas, lower pressures and lower growing times determined the formation of cylinder-shape nanowires ("straight wires") uniformly distributed on the carbon paper fibres forming a high interconnected network with lengths over 5µm (Fig. 1) and diameters ranging between 200-300 nm and density varying from 2 mg cm^{-2} to 5 mg cm^{-2}. The use of SiH$_4$ mixed with Ar determined a "coral like" (Fig. 2) morphology. The third set of parameters, characterized by high flux and higher SiH$_4$/Ar ratio, gave an intermediate morphology with both features present (data not shown).
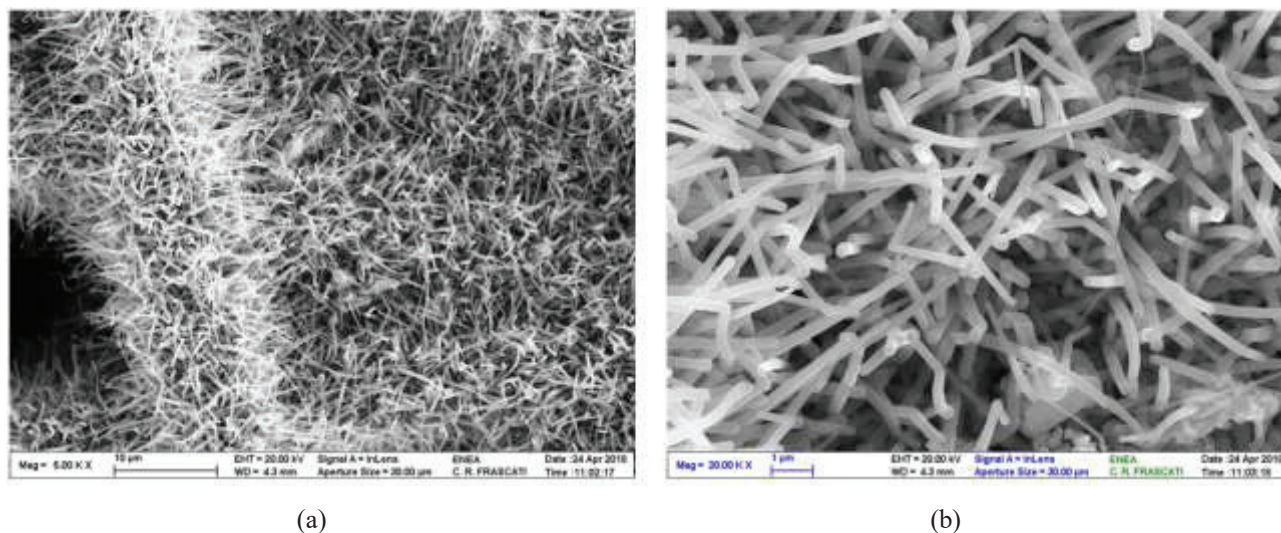

(a)   (b)

FIGURE 1. SEM images of straight wires Si-NWs at 5kx (a), 20kx magnification (b).

(a)   (b)
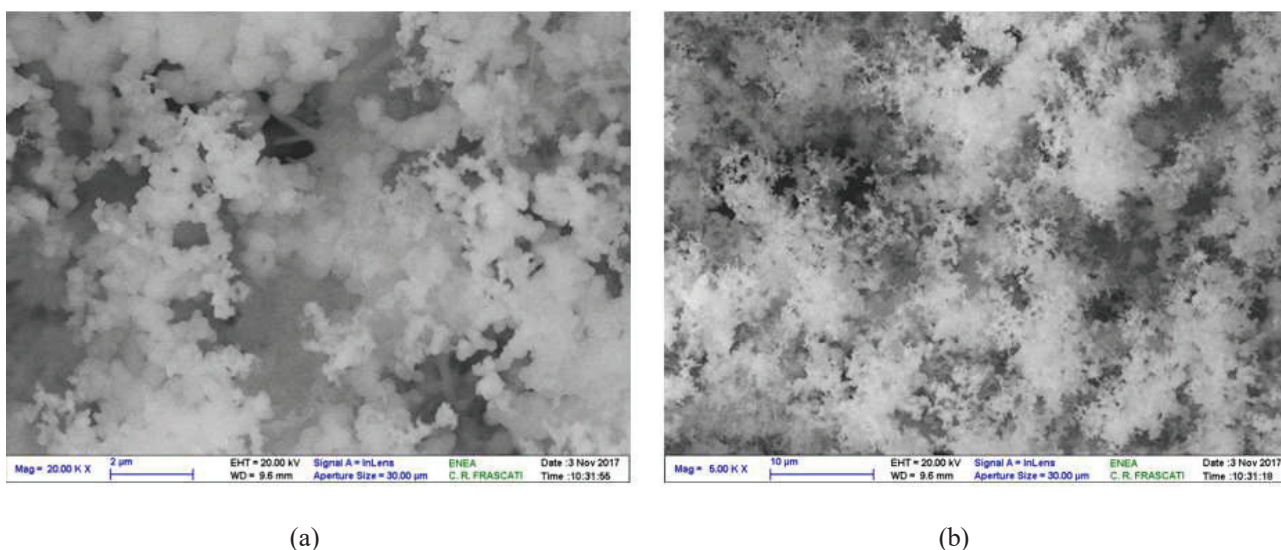
FIGURE 2. SEM images of coral like Si-NWs at 5kx (a), 20kx magnification (b).

The structural analysis of all the typologies of Si-NWs showed the same diffraction pattern and a typical spectrum is reported in Fig. 3. This diffractogram is characterized by a very high intensity peak located at about 26.4 2θ and a second at 54.5 2θ that can be ascribed to the carbon paper substrate (PDF card N° 00-041-1487); all the other peaks can be attributed to synthetic silicon (PDF card N° 00-027-1402).
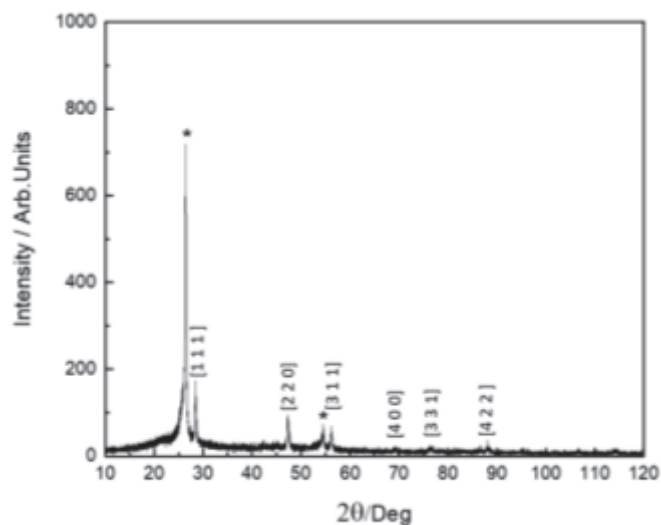
FIGURE 3. XRD pattern of the silicon nanowires deposited on carbon paper substrate. The peaks belonging to the carbon substrate are asterisked.

Preliminary galvanostatic cycles were performed on all the morphologies obtained. Coral-like and intermediate morphologies didn't lead to stable and significative results, while the Si-NWs showed a good reproducibility, promising results and were selected for further electrochemical characterization. A cyclic voltammetry (CV) was carried out to evaluate the electrochemical window before to perform the galvanostatic tests. CV was performed at slow rate (0.05 mV s-1) in the voltage range 0.005-2.000 V and Fig. 4 reports the first two scan cycles. The lithiation starts at about 0.9 V: the current strongly increases at 250 mV (peak A), a further variation of the curve slope is observed around 150 mV and the complete lithiation peak, that normally occurs below 50 mV, was detected at 10 mV (peak B). During the second scan cycle the peak A shifts to 140 mV, whereas the peak B is observed at the same value (10 mV). In the first delithiation cycle, two peaks can be observed at 280 mV (peak C) and at 580 mV (peak D). During the second cycle the peak D shifts to 620 mV.

As reported in literature [11], the peak A is attributed to the lithiation of the amorphous Si shell and the peak B refers to the complete lithiation of the crystalline Si core. The peak D can be attributed to contemporaneous de-lithiation process of the coexisting crystalline Li15Si4 phase and the amorphous LixSi phase. Cui and co-workers explain the shifting of the second scan peaks with a partial amorphization of the crystalline core due to the lithiation forced to very low voltage values.
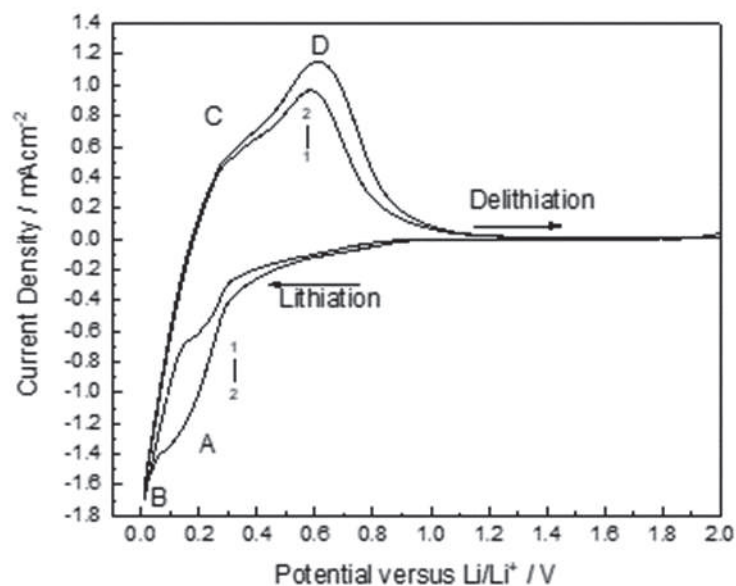

FIGURE 4. CVs of Si-NWs electrode carried out at 0.05 mV s^{-1} between 2.000 and 0.005 V.

From the result of the CV, to ensure and test the complete lithiation of silicon, the lower cut-off voltage for the galvanostatic cycling was selected at 0.005 V whereas the higher cut-off voltage was fixed at 0.900 V. To allow the

formation of a stable SEI on the silicon surface, the first charge-discharge cycle was performed at very low current (C/40). In the subsequent cycles the current was doubled (C/20). A galvanostatic test was carried out on the bare carbon paper electrode to evaluate a possible substrate contribution to the total electrode capacity. From this test it was found that the substrate contribute is as low as 60 mAh g-1. The voltage profiles recorded during the galvanostatic cycling are shown in Fig. 5a. During the first discharge cycle the voltage rapidly decreases to 0.300 V then it smoothly declines down to 0.150 V; after that a voltage plateau is observed extending from 500 mAh g-1 up to 2500 mAh g-1. In the first instants of the charge process a large voltage hysteresis is observed: the voltage rises from 0.005 V (end discharge voltage) up to 0.150 V. It is not possible to identify a clear voltage plateau as the voltage increases somewhat steadily with time. When the cell voltage has reached the condition of end of charge the capacity released by the electrode is equal to 2357 mAh g-1. The subsequent discharge cycles are different from the first but similar to each other. The cell voltage quickly reaches a value close to 0.300 V and then declines with a constant slope until it reaches the end of the discharge.

As the number of cycles progresses, there is a gradual decrease in capacity and after 50 cycles the electrode is able of discharging only one tenth of the capacity exhibited during the first discharge cycle. The evolution of the specific capacity for the alloying and dealloying processes and the charge coefficient as function of the cycle number for the first ten cycles is reported in Fig. 5b. A linear decrease of the specific capacity is observed upon cycling: the average capacity fading is about 5% per cycle. On the other hand, the charge coefficient, namely the ratio between the amount of charge used to fully recharge the battery and the drawn charge, improves with cycling and increases from 95% up to 100% in few cycles maintaining this value in following cycles. The very good reversibility of the alloying/dealloying process can be attributed to the formation of a stable and compact SEI. It has also to be pointed out that the charge/discharge ratio is quite high even at the first cycle (95%), showing that the amount of energy used for SEI formation is relatively low.
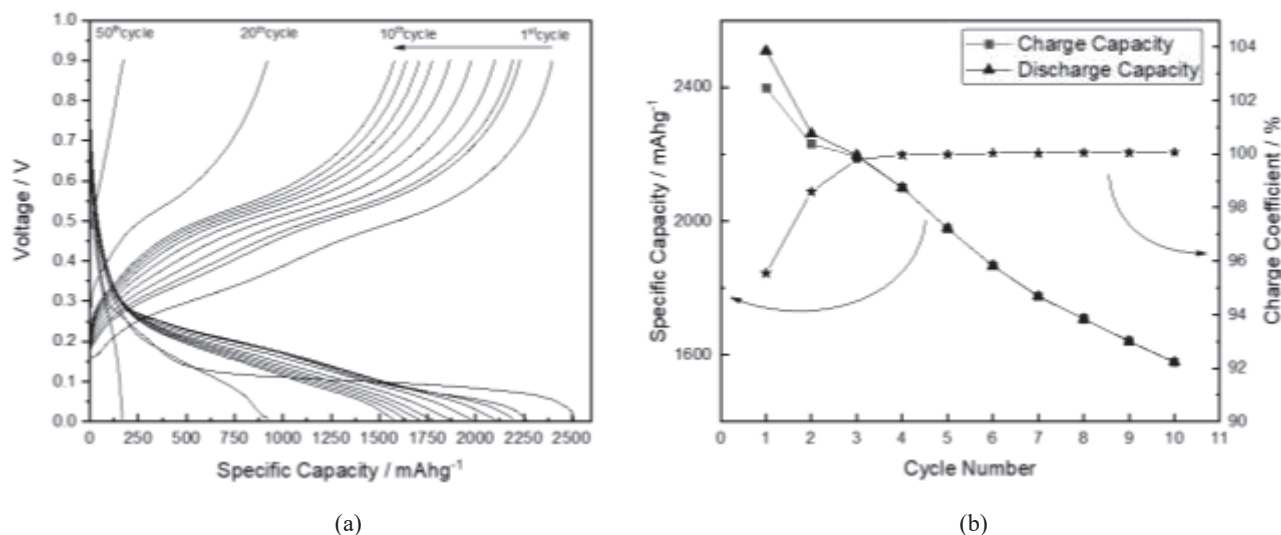

(a)   (b)

FIGURE 5. (a) Voltage profiles as a function of the specific capacity, (b) Specific capacity and charge coefficient for the first ten cycles. The cell cycled at C/20 in the potential range 0.005-0.900V after a first cycle performed at C/40 in the same voltage range.

To better understand the reason for the severe capacity fading, morphological analysis was performed on the cycled electrodes; Fig. 6 shows a SEM image of the electrode after 50 charge/discharge cycles. The active material appears partially or completely fragmented and detached from the substrate leaving the carbon fibers visible, where the Si-NWs are still visible even though enclosed inside a thick layer of SEI. The chemical composition of the carbon fibers, the silicon nanowires and the residue has been confirmed by a single-spot EDX analysis (data not shown). Post-mortem analysis also showed the presence of a silicon layer of about 2 μm in thickness that partially embedded the Si-NWs (Fig.7). The same layer was observed also in a pristine sample. The presence of this thick silicon layer, underlying the Si-NWs, undermines the advantages of the nanostructures and could be responsible for the severe capacity fading exhibited by the electrode. As indeed reported in literature, the volume expansion in bulk silicon is the main responsible for capacity fading and, in these samples, could account for the severe fragmentation and pronounced capacity fading.
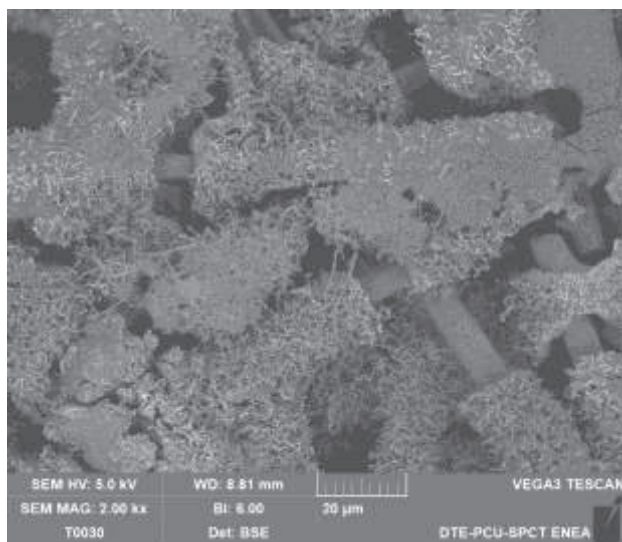
FIGURE 6. Post-mortem backscattered electron SEM image: bare carbon fibers are clearly visible.
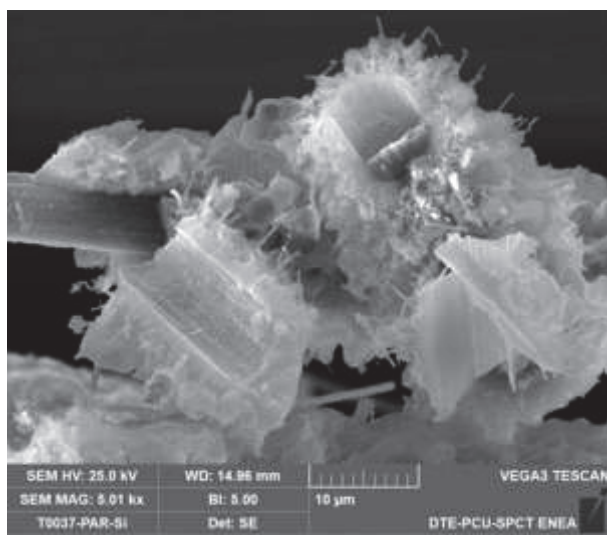

FIGURE 7. Post-mortem secondary electrons SEM images: Straight Si-NWs on a thick continuous silicon layer; detached chunks show the carbon paper imprinted on the inside.

CONCLUSIONS

Carbon paper was found to be a suitable substrate for the growth of Si-NWs. Compared to other substrates, the carbon paper determines a widespread Si-NWs growth and allows to reach very high silicon densities. Furthermore, by varying the growth conditions such as temperature, flux and concentration of the silane gas, it is possible to select the morphology from "coral" to "wire". Upon electrochemical cycling the Si-Nws show a high capacity in the first cycle (2500 mA g-1), a very low value of the irreversible capacity (about 5% of discharged capacity) and a charge coefficient that approaches 100% after only three cycles. Despite these promising results, the use of these wires as negative electrodes for lithium batteries has not been suitable for practical applications since they present a pronounced loss of capacity with cycling. This capacity fading can be attributed to the presence of a silicon layer between the Si-NWs and the current collector substrate. The lithiation process of this layer could be responsible for the loss of contact between the substrate and the active material, probably due to the mechanical stresses exerted by the alloying/dealloying processes as it happens for bulk silicon. In order to avoid the unwanted silicon layer, further investigations on the influence of growth parameters on the nanostructure morphology, are necessary to improve electrochemical performance especially in terms of capacity retention, cyclability and cycle life. The use of carbon paper as substrate for the fabrication anodes for Li-ion battery could be highly advantageous both for the low contribute of carbon paper on the overall weight of the electrode and for the high achievable density of Si-NWs.

REFERENCES

1. U. Kasavajjula, C. Wang, A.J. Appleby, "Nano-and bulk-silicon-based insertion anodes for lithium-ion secondary cells", *J. Power Sources* **163** (Elsevier, 2007), pp.1003-1039.
2. B. Scrosati, J. Garche, Review "Lithium batteries: Status, prospects and future", *J. Power Sources* **195** (Elsevier, 2010), pp.2419-2430.
3. N. Nitta, F. Wu, J.T. Lee, G. Yushin, Li-ion battery materials: present and future, *Mater. Today* **18** (Kidlington, 2015), pp. 252-264,
4. L.F. Nazar, O. Crosnier, Chapter 4 "Anodes and Composite Anodes: An Overview", in *Lithium Batteries Science and Technology*, edited by Golam-Abbas Nazri and Gianfranco Pistoia, (Springer, 2009), pp.112-115.
5. M.R. Zamfir, H.T. Nguyen, E. Moyen, Y.H. Lee, D. Pribat, "Silicon nanowires for Li-Based battery anodes: a review", *J. Mater. Chem. A* **1** (RSC Publishing, 2013), pp.9566-9586.
6. R. Teki, M.K. Datta, R. Krishnan, T.C. Parker, T.M. Lu, P.N. Kumta, N. Koratkar, "Nanostructured Silicon Anodes for Lithium Ion Rechargeable Batteries", *Small* **5** (Wiley-VCH, 2009), pp.2236-2242.
7. J.R. Szczech, S. Jin, "Nanostructured silicon for high capacity lithium battery anodes", *Energy Environ Sci.* **4** (RSC, 2011), pp.56-72.
8. H.C. Shina, J.A. Cornob, J.L. Goleb, M. Liua, "Porous silicon negative electrodes for rechargeable lithium batteries", *J. Power Sources* **139** (Elsevier, 2005), pp.314–320.
9. H. Wu, G. Zheng, N. Liu, T. J. Carney, Y. Yang, Y. Cui, "Engineering Empty Space between Si Nanoparticles for Lithium-Ion Battery Anodes", *Nano Lett.* **12** (ACS Publications, 2012), pp.904−909.
10. V. Schmidt, J. V. Wittemann, S. Senz, U. Gösele, "Silicon Nanowires: A Review on Aspects of their Growth and their Electrical Properties", *Adv. Mater.* **21** (Wiley-VCH, 2009), pp.2681-2702.
11. L.F. Cui, R. Ruffo, C.K. Chan, H. Peng, Y. Cui, "Crystalline-Amorphous Core-Shell Silicon Nanowires for High Capacity and High Current Battery Electrodes", *Nano Lett.* **9** (ACS, 2009), pp.491-495.
12. T. Kennedy, M. Brandon, F. Laffir, K.M. Ryan, "Understanding the influence of the electrolyte on the electrochemical performance and morphology evolution of the silicon nanowirebased lithium-ion battery anodes", *J. Power Sources* **359** (Elsevier, 2017), pp. 601-610.
13. A.L. Michen, B.S. Parimalam, M. Leskes, R.N. Kerber, T. Yoon, C.P. Grey, B. L. Lucht, "Fluoroethylene Carbonate and Vinylene Carbonate Reduction: Undestanding Lithium-Ion Battery Electrolyte Additives and Solid Electrolyte Interphase Formation", *Chem. Mat.* **28** (ACS Publications, 2016), pp. 8149-8159.
14. V. Etacheri, O. Haik, Y. Goffer, G.A. Roberts, I.C. Stefan, R. Fasching, D. Aurbach, "Effect of Fluoroethylene Carbonate (FEC) on the Performance and Surface Chemistry of Si-Nanowire Li-Ion Battery Anodes", *Langmuir* **28** (ACS Publications, 2012), pp.965–976.
15. E. Peled, F. Patolsky, D. Golodnitsky, K. Freedman, G. Davidi, D. Schneier, "Tissue-like Silicon Nanowires-Based Three-Dimensional Anodes for High-Capacity Lithium Ion Batteries", *Nano Lett.* **15** (ACS Publications, 2015), pp.3907-3916.
16. R.S. Wagner, W.C. Ellis, "Vapor-Liquid- Solid Mechanism of Single Crystal Growth", *Appl. Phys. Lett.* **4**, (AIP, 1964), pp.89-90.
17. E. I. Givargizov, "Fundamental aspects of VLS growth", *J. Cryst. Growth* **31**, (Elsevier, 1975), pp.20–30.
18. P.P Prosini, C. Cento, A. Rufoloni, F. Rondino, A. Santoni, "A lithium ion battery based on LiFePO$_4$", *Solid State Ion.* **269** (Elsevier, 2015), pp.93-97.
19. J. Arbiol, B. Kalache, P.R. Cabarrocas, J.R. Morante, A. Fontcuberta i Morral, "Influence of Cu as a catalyst on the properties of silicon nanowires synthesized by the vapour–solid–solid mechanism", *Nanotechnology* **18**, (IOP Publishing, 2007), pp.1-8.
20. J.L. Lensch-Falk, E.R. Hemesath, D.E. Perea, L.J. Lauhon, "Alternative catalysts for VSS growth of silicon and germanium nanowires", *J. Mater. Chem.* **19**, (RSC, 2009), pp.849-857.